J. Am. Ceram. Soc., 70 [5] 323-28 (1987)

Drying Shrinkage Mechanisms in Portland Cement Paste

WILL HANSEN*

Department of Civil Engineering, The University of Michigan, Ann Arbor, Michigan 48109-2125

The shrinkage mechanisms of portland cement paste were investigated from shrinkage, weight loss, and pore structure measurements using nitrogen sorption and mercury intrusion porosimetry (MIP). Thin samples (2.3 mm) of well-hydrated (165 d) pastes of 0.4 and 0.6 water-to-cement (W/C) ratios were dried directly from saturated surface dry state to 75%, 50%, 11%, and 0% relative humidity (rh). From equilibrium shrinkage vs calculated increase in surface free energy curves two active stress mechanisms were identified. The Gibbs-Bangham (surface free energy) effect is the major stress mechanism, which is active in the entire rh range investigated, whereas the capillary stress effect is active above 25% rh. From elastic modulus calculations it can be concluded that true Gibbs-Bangham shrinkage accounts for only 33% of total first drying shrinkage. Thus nearly 67% of first drying shrinkage may be due to a decrease in interlayer spacing caused by Gibbs-Bangham and capillary induced stresses. Further, nitrogen measures the true external surface area, and total external pore volume can be obtained from combined measurements using nitrogen sorption and MIP.

I. Introduction

DRYING shrinkage, defined as the time-dependent deformation due to loss of water at constant temperature and relative humidity (rh), is a characteristic property of portland cement paste and concrete. Despite extensive investigation into the origin of shrinkage, this property is not well understood. The four most prominent shrinkage mechanisms that have been proposed are surface free energy,[1-7] capillary tension,[1,2,6,8,9,12] movement of interlayer water,[3-5,7,8,11,12] and disjoining pressure.[1,2,7,10,11] There is at present no unified theory which adequately explains the reversible and irreversible drying shrinkage behavior of paste or concrete over the entire relative humidity region. It is generally perceived that more than one mechanism is involved.[1-12] A better understanding of the shrinkage phenomena is necessary to provide a sound basis for accurate prediction of paste and concrete shrinkage and for developing methods which would reduce or eliminate the adverse property of drying shrinkage.

In the present study the shrinkage and weight loss vs relative humidity are investigated for different W/C ratio pastes together with pore structure measurements using nitrogen sorption and MIP.

II. Experimental Procedure

Type I portland cement pastes were cast into slabs using a modified procedure derived from that of Parrott *et al.*[13] The W/C ratios used were 0.4 and 0.6. To minimize sedimentation the pastes were rotated in a sealed container at 10 rpm and allowed to partially hydrate before being cast. Once they had a creamy consistency they were cast in Plexiglas* molds and continued to rotate until after time of final set. After 24 h the slabs were demolded and cured at room temperature (24 ± 3°C) for 165 d in an airtight container filled with lime-saturated water.

The shrinkage specimens were cut from the slab into 2.3-mm thickness and 76-mm length. The specimens were fitted at each end with a stainless steel clamp having a spherical slot at the center to facilitate a ball seating in the dial gauge. Shrinkage readings were reproducible to $\pm 5 \times 10^{-6}$ strain. Stability of the dial gauge was checked periodically by a reference invar bar. Long-term drift was within 10×10^{-6} strain. The shrinkage specimens were dried in desiccators conditioned at 75%, 50%, and 0% rh using aqueous solutions of sulfuric acid. The rh was maintained by stirring the solutions continuously during the entire period of drying. An rh of 0% corresponds to drying over vapor pressure of concentrated sulfuric acid. The desiccators were kept in an environmental chamber in which the temperature was maintained at 24 ± 0.5°C. Shrinkage and weight changes were measured on the same specimens. The weight changes were measured† with a reproducibility of 0.02 mg. For each measurement duplicate specimens were used.

Before pore structure measurements, thin specimen slices were solvent replaced in methanol for about 2 weeks prior to drying at 0% rh for 4 d. Solvent replacement was used in order to preserve the original external pore structure. Litvan[14] showed that there was better agreement between the surface areas obtained by water and nitrogen if the nitrogen surface area was measured on solvent-replaced samples.

The pore structure was measured using a mercury intrusion porosimeter with a capacity of 414 MPa (60 000 psi)‡ and a nitrogen surface area analyzer.§ The Washburn equation was used to calculate pore volume vs diameter from MIP results. A mercury surface tension of 480×10^{-3} N/m and a contact angle of 140° were used. Nitrogen adsorption isotherms were obtained by means of the dynamic method using He as a carrier gas. From these the volume (V) vs statistical thickness (t) curves were constructed using the reference t curve of Cranston and Inkley.[15]

III. Results and Discussion

(1) Drying Shrinkage and Weight Loss vs Time Curves

The curves shown in Figs. 1(*A*) and (*B*) illustrate first drying shrinkage and weight loss, respectively, vs drying time at 75%, 50%, 11%, and 0% rh. The data shown are for the 0.6 W/C portland cement paste. The curves are typical for the two systems investigated. Each curve is the average of the results obtained from two companion specimens. The variations in shrinkage and weight loss between companion specimens were within 0.02% and $0.004(\Delta W/W_{SSD})$, respectively, for drying at 75%, 50%, and 11% rh, whereas drying at 0% rh resulted in variations within 0.04% for shrinkage and 0.008 for relative weight loss. Both shrinkage and weight loss were obtained on each specimen.

The results illustrate that true shrinkage and weight loss equilibrium are not reached within the time period investigated (200 d). The exceptions are the weight loss curves for drying at 11% and 0% rh, where equilibrium is reached within 7 and 14 d, respectively. The lack of equilibrium within an extended drying period agrees well with results reported by Parrott and Young.[6] They observed a similar behavior on second drying although the shrinkage was considerably less. It is reasonable to assume that approximate shrinkage equilibrium is reached for thin specimens (2.3 mm) within a drying period of 200 d, since the shrinkage values extrapolated out to several years will not exceed the 200-d value by more than a few percent.

Received April 3, 1985; revised copy received May 6, 1986; approved November 26, 1986.

*Member, the American Ceramic Society.

*Rohm and Haas Co., Philadelphia, PA.

†Mettler balance, Mettler Instrument Corp., Hightstown, NJ.

‡Autoscan-60, Quantachrome Co., Syosset, NY.

§Quantasorb, Quantachrome Co.

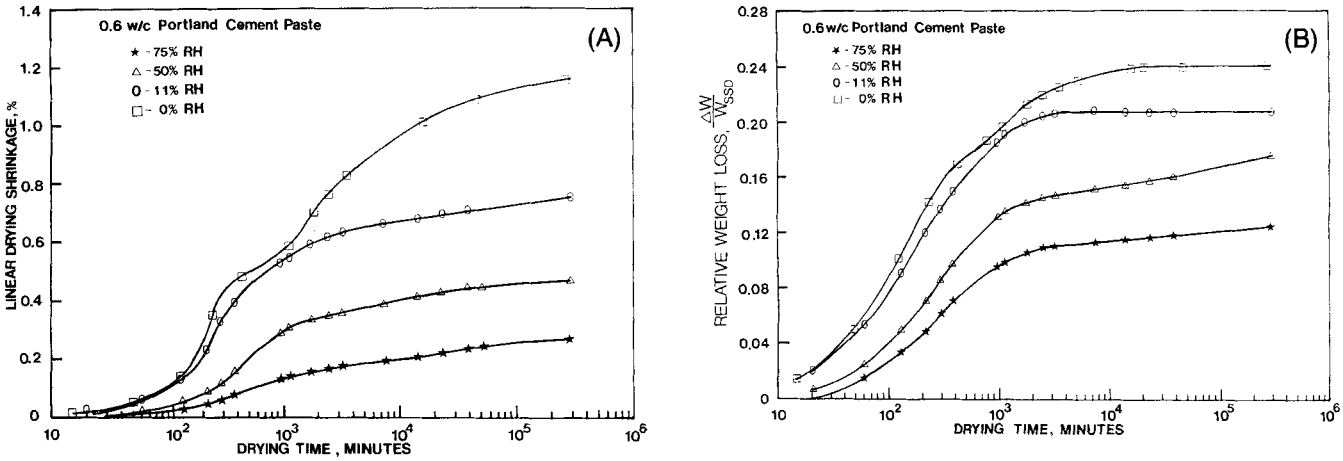

Fig. 1. (*A*) Curves of shrinkage vs drying time upon first drying of 0.6 W/C ratio portland cement paste. (*B*) Curves of weight loss vs drying time upon first drying of 0.6 W/C ratio portland cement paste.

(2) Dynamic Shrinkage Weight Loss Curves

The dynamic shrinkage weight loss curves, which are based on transient (i.e., nonequilibrium) shrinkage and weight loss values, are shown in Figs. 2(*A*) and (*B*) for the 0.4 and 0.6 W/C ratio pastes, respectively. The curves were constructed from concomitant shrinkage and weight loss results as shown in Fig. 1 for the 0.6 W/C ratio paste. The curves at 75%, 50%, 11%, and 0% rh combine to form a single continuous shrinkage vs weight loss curve for each paste spanning the rh range between 100% and 0%. This curve includes equilibrium shrinkage values. This is in good agreement with results by Roper[16] and Verbeck and Helmuth.[17] It shows that the duration of time a specimen is subjected to internal shrinkage stresses due to drying does not influence shrinkage results. As evident from Fig. 1(*B*) the rates of moisture loss increase with drying at lower rh. Thus an increase in moisture gradient within a specimen is expected. This does not seem to affect the dynamic shrinkage weight loss curves (Figs. 2(*A*) and (*B*)) of thin specimens. Thus true material shrinkage can be obtained on thin specimens. This is of prime importance for testing shrinkage mechanisms and for predicting drying shrinkage of concrete from thin specimens.

The continuous curves in Figs. 2(*A*) and (*B*) are characterized by an increase in shrinkage vs weight loss with increasing water loss, except for the 0.6 W/C ratio paste, which has a region of lower shrinkage vs weight loss close to the equilibrium values for shrinkage and weight loss at 50% rh. This is in good agreement with results by Roper.[16] This region suggests that more than one shrinkage mechanism is active in the rh range between 100% and 0%.

(3) Equilibrium Shrinkage vs Relative Humidity Curves

The continuous dynamic shrinkage weight loss curves (Figs. 2(*A*) and (*B*)) are helpful when constructing the equilibrium shrinkage vs relative humidity curves based on measurements at a few relative humidities, since they show that there is a continuous increase in shrinkage. Thus shrinkage vs rh would increase continuously as well. The equilibrium values from shrinkage vs time curves at 75%, 50%, 11%, and 0% rh were used to construct the equilibrium shrinkage vs rh curves for the 0.4 and 0.6 W/C ratio pastes. The curves are shown in Fig. 3. They were obtained by joining the shrinkage values through smooth curves characterized by opposite curvature in the two rh ranges of 0% to 11% and 50% to 100%. The shape of the curves as well as the shrinkage

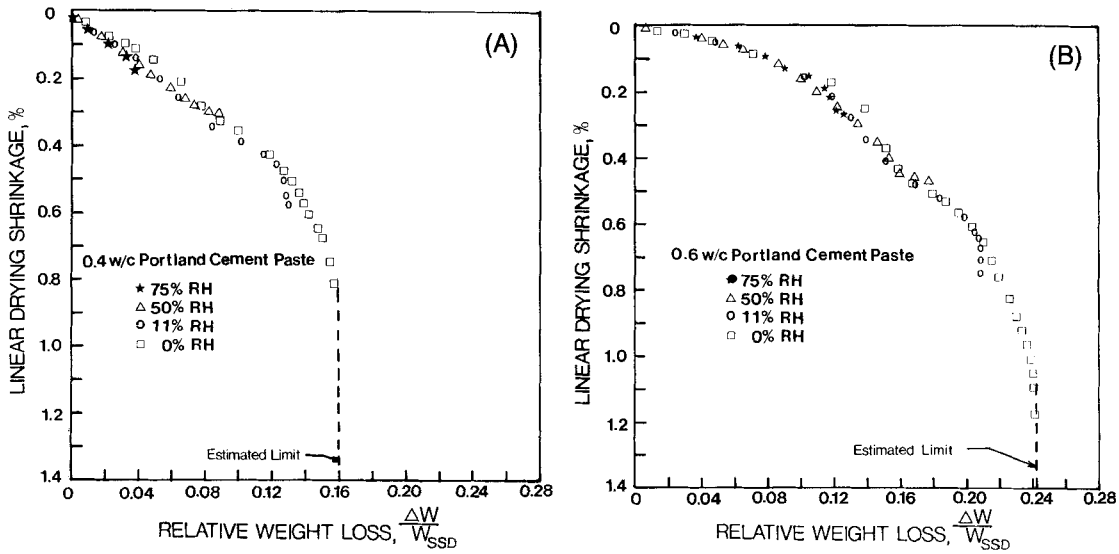

Fig. 2. (*A*) Dynamic shrinkage weight loss curves of 0.4 W/C ratio paste upon first drying at 75%, 50%, 11%, and 0% rh. (*B*) Dynamic shrinkage weight loss curve of 0.6 W/C ratio paste upon first drying at 75%, 50%, 11%, and 0% rh.

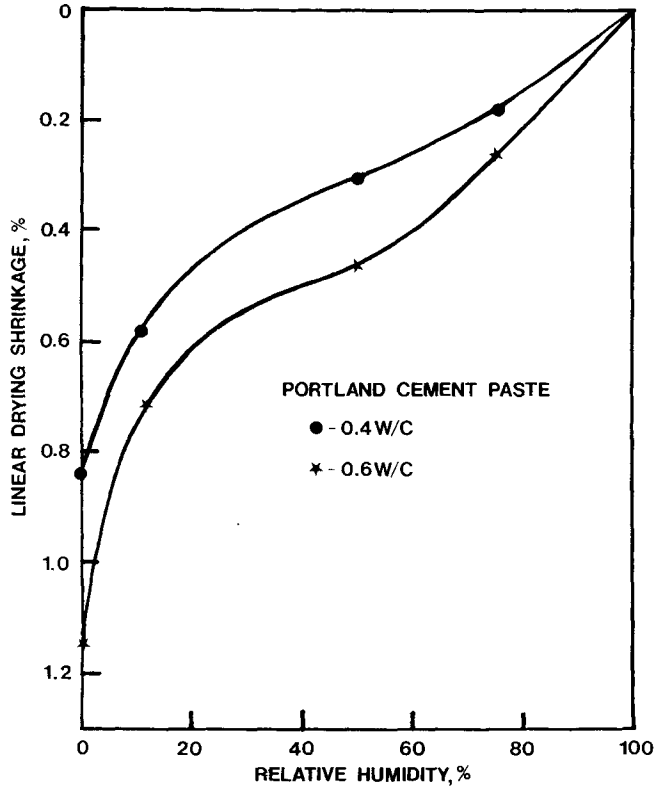

Fig. 3. Equilibrium first drying shrinkage vs relative humidity curves of 0.4 and 0.6 W/C ratio pastes hydrated for 165 d before drying for 200 d at 75%, 50%, 11%, and 0% rh.

values are in good agreement with those reported by other investigators.[5,17-19]

(4) Gibbs-Bangham Stress-Induced Shrinkage

Bangham *et al.*[20] were able to predict the expansion of a high-surface-area material such as charcoal by means of an empirical equation

$$\Delta l/l = \lambda \Delta F \tag{1}$$

where $\Delta l/l$ is the expansion strain, ΔF is the calculated decrease in surface free energy (N/m), and λ is a constant (cm/N). It was shown by Bangham and Razouk[21] that the decrease in surface free energy ($F_0 - F$) of a solid is equivalent to the decrease in surface tension ($\gamma_0 - \gamma$) and calculated increase in spreading pressure, π, using the Gibbs adsorption equation[22]

$$\pi = \Delta F = F_0 - F = \gamma_0 - \gamma$$
$$= \frac{10^{-3}RT}{\bar{V}} \int_0^P \frac{V_l}{S} d(\ln P) \quad (\text{N/m}) \tag{2}$$

where R is the gas constant (N·cm/(mol·K)), T is the absolute temperature (K), $\bar{V}$ is the molar volume of adsorbed liquid (cm^3/mol), S is the specific surface area of the solid (cm^2/g), and V_l is the volume of adsorbed liquid (cm^3/g). The validity of Eq. (2) is based on the assumption that the adsorbed molecules behave like a two-dimensional gas. It is convenient to use relative pressure P/P_0 instead of the absolute pressure P. Equation (2) can be rearranged to incorporate this. Thus

$$\Delta F = \frac{10^3RT}{\bar{V}} \int_{P_1/P_0}^{P_2/P_0} \frac{V_l}{S} d(\ln (P/P_0)) \quad (\text{N/m}) \tag{3}$$

where $P_1/P_0 < P_2/P_0$. To integrate Eq. (3) the relationship between V_l/S vs relative pressure (P/P_0) at equilibrium must be known. V_l and S can be conveniently obtained from nitrogen sorption. Nitrogen is preferred over water because the complete

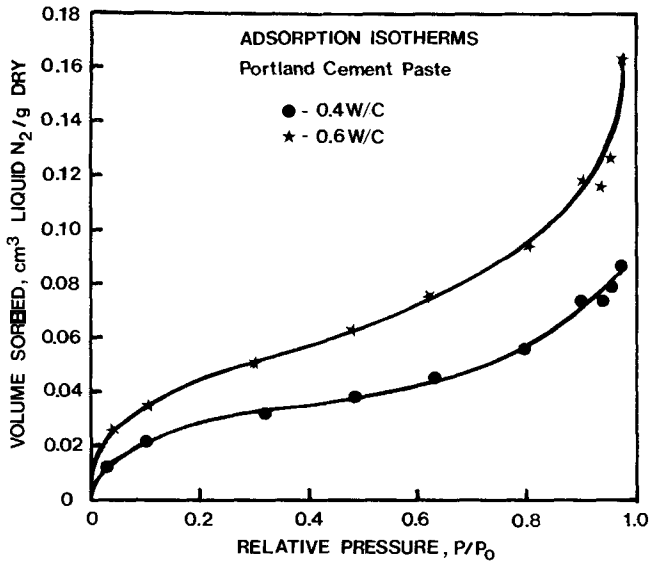

Fig. 4. Nitrogen adsorption isotherms of 0.4 and 0.6 W/C ratio pastes hydrated for 165 d and solvent replaced.

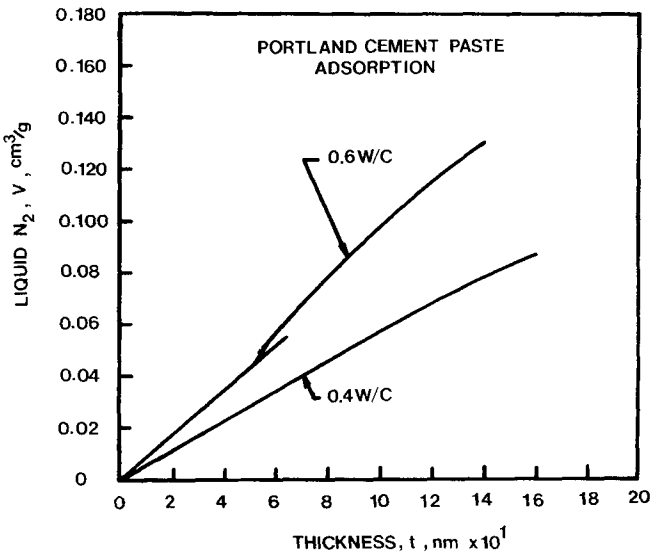

Fig. 5. Nitrogen *V-t* curves of 0.4 and 0.6 W/C ratio pastes hydrated for 165 d and solvent replaced.

isotherm can be obtained more quickly. Each point on the isotherm is obtained within 1 h when nitrogen is used as compared to several days for water (Fig. 1(*B*)). In addition the simultaneous removal of interlayer water at low rh makes it difficult to calculate the external surface area. The only drawback to the use of nitrogen is that the paste has to be predried at 0% rh before sorption measurements, which in turn would alter the original pore structure. This has been overcome in the present study by means of solvent replacement.

The nitrogen adsorption isotherms of the 0.4 and 0.6 W/C ratio pastes are shown in Fig. 4. They were used together with the reference t curve of Cranston and Inkley[15] to construct the *V-t* curves shown in Fig. 5. The total external surface area was obtained from the slope of the initial straight line portion of the *V-t* curve which goes through the origin. Values of 53 and 83 m^2/g were obtained for the 0.4 and 0.6 W/C ratio pastes, respectively.

For the 0.4 W/C ratio paste pore filling due to multilayer sorption occurs at t values greater than about 1.2 nm. Thus at t values greater than 1.2 nm the remaining surface area is continuously

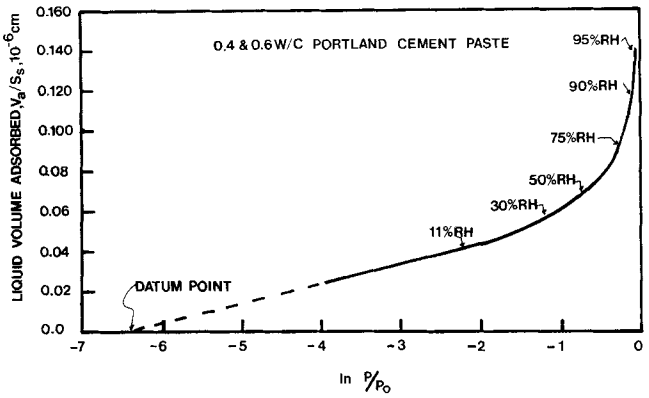

Fig. 6. Normalized volume adsorbed vs ln (P/P_0) of 0.4 and 0.6 W/C ratio paste as obtained from *V-t* analysis.

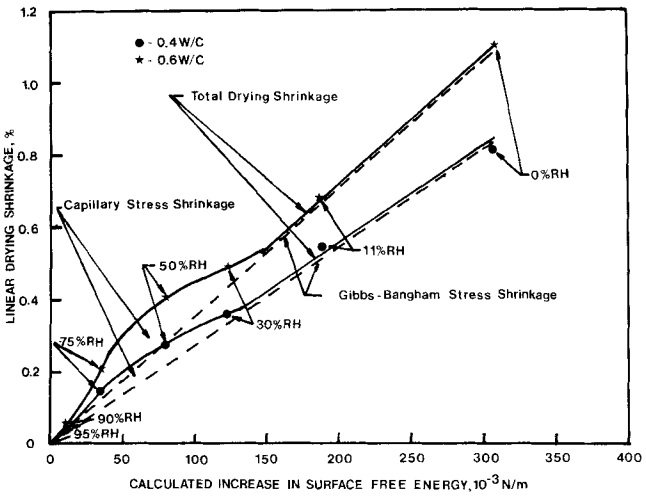

Fig. 7. First drying shrinkage of 0.4 and 0.6 W/C ratio pastes vs calculated increase in surface free energy.

diminished. Therefore the surface area S in Eq. (3) is a variable for rh values greater than about 90%. This parameter is therefore kept inside the integration sign. No capillary condensation occurs in the 0.4 W/C ratio paste in the pore diameter range accessible to nitrogen, since there is no upward deviation in the slope of the *V-t* curve compared to that of the initial straight line going through the origin. Capillary condensation does occur in the 0.6 W/C ratio paste. But the contribution to the overall pore volume accessible to nitrogen is small.

Assuming that the pore structure subjected to multilayer sorption is similar for the two pastes the term V_l/S vs ln (P/P_0) is the same as well. This curve is illustrated in Fig. 6. The datum point which corresponds to zero adsorbed liquid was extrapolated from the linear relationship of V_l/S vs ln (P/P_0) in the low rh range. The location of this datum point is important because it influences the calculated surface free energy at low rh. The datum point was found at -6.4 on the ln (P/P_0) axis. This value agrees reasonably well with a value of -5.15 obtained by Hiller[24] from a study on porous Vycor[¶] glass.

The calculated decrease in surface free energy based on Eq. (3) is shown in Table I for different rh segments.

[¶]Corning Glass Works, Corning, NY.

Table I. Calculated Decrease in Surface Free Energy of 0.4 and 0.6 W/C Ratio Pastes at Incremental Increases in Relative Humidity

rh (%)	ΔF ($\times 10^{-3}$ N/m)
0–11	119
11–30	67
30–50	43
50–75	44
75–90	26
90–95	9.6

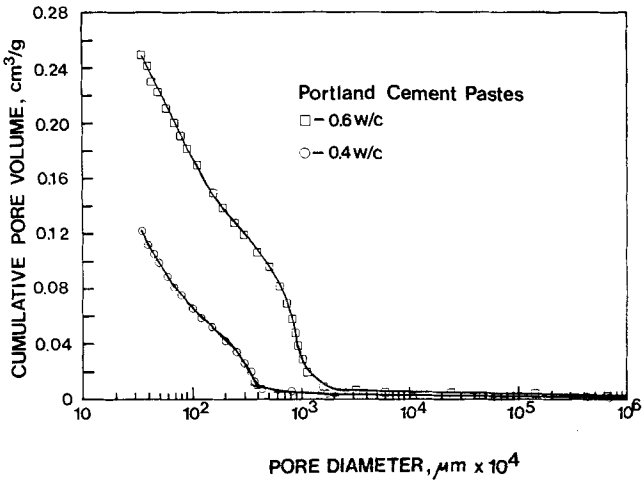

Fig. 8. Cumulative pore size distribution curves by MIP of 0.4 and 0.6 W/C ratio portland cement pastes hydrated for 165 d, then solvent replaced.

By means of *V-t* analysis the adsorbed water volume at equilibrium can be separated from the capillary water. The external surface area can be determined as well. Therefore, the surface free energy can be estimated at any relative humidity range. However, in order to test the Gibbs-Bangham equation on cement paste subjected to first drying, the effects of irreversibility on equilibrium shrinkage must be known. In the present study equilibrium shrinkage is not affected by irreversible effects because thin specimens are used. Helmuth and Turk[25] showed that the irreversible shrinkage of thin specimens is <15% of total shrinkage within 1 d of drying. Within this period nearly 70% of the estimated equilibrium shrinkage has occurred for specimens dried within the rh range of 11% and higher (Fig. 1(*A*)). In addition most of the irreversible shrinkage develops after the first day of drying[6,25] such that it may account for 60% or more of total final drying shrinkage following long-term drying. Thus the irreversible and total shrinkage develop differently. Therefore, first drying shrinkage of thin specimens is not affected by irreversible effects. Consequently it is advantageous to test the Gibbs-Bangham mechanism on first drying since testing a completely stabilized paste (i.e., no irreversible effects) would require drying for a year or more. However, it also means that true Gibbs-Bangham shrinkage would be considerably overestimated by using first drying shrinkage results.

The Gibbs-Bangham equation, which is normally tested on adsorption (i.e., rewetting) can also be used on drying. This is more convenient in the present study. Figure 7 illustrates total shrinkage at equilibrium obtained from Fig. 3 vs calculated increase in surface free energy from Table I for the 0.4 and 0.6 W/C ratio pastes. The origin of the curves corresponds to 95% rh. It was chosen because 95% rh represents the upper limit of *V-t* analysis. The shrinkage values at 95% rh were then subtracted from shrinkage at 75%, 50%, 30%, 11%, and 0% rh. According to Fig. 7 it is now possible to separate total shrinkage into two components since for the most part both curves follow a linear relationship between

shrinkage and surface free energy. This is shown by the dotted line which illustrates that the majority of first drying shrinkage is Gibbs-Bangham stress induced. At relative humidities above 30% an additional stress mechanism is active. However, the contribution to overall shrinkage from this mechanism is considerably less than the Gibbs-Bangham stress shrinkage. It accounts for nearly 33% of total shrinkage at 50% rh for the 0.6 W/C ratio paste but only 15% of the total shrinkage for the 0.4 W/C ratio paste.

A linear relationship between length change and change in surface free energy, as described by the two dotted lines in Fig. 7, is not conclusive evidence of Gibbs-Bangham shrinkage.[1,2] According to this mechanism the dimensional change is due to compression of a high-surface-area solid. This can be evaluated from λ, which, according to Bangham and Maggs,[26] is related to the elastic modulus of the solid by the following relationship:

$$E = \rho S_s/\lambda \quad \text{(MPa)} \tag{4}$$

where E is the elastic modulus of the solid, S_s is the specific surface area of the solid in m^2/g, ρ is the solid density in g/cm^3, and λ is the slope of the dimensional change vs calculated change in surface free energy (m/N). It can be shown from results on porous Vycor glass that Eq. (4) does not accurately predict the elastic modulus of the solid. From results of S_s, ρ, and λ obtained by other researchers,[24,27] an average value of 37 931 MPa (5.5×10^6 psi) is calculated for Vycor glass. In these calculations a value of 117 m^2/g was used for S_s[27] together with a density value of 2.18 g/cm^3 (Ref. 24) and an average value of 7.22×10^{-3} m/N based on reported values of 5.333×10^{-3} m/N (Ref. 24) and 9.1×10^{-3} (Ref. 27). The measured values for elastic modulus of the solid Vycor glass fall in the range of 59 310 MPa (8.6×10^6 psi) to 77 931 MPa (11.3×10^6 psi) with an average value of 68 621 MPa (9.95×10^6 psi).[28] Thus Eq. (4) can be used for comparisons assuming that it predicts a value for the elastic modulus which is 55% of the true value. Therefore, if the length change described by the dotted lines in Fig. 7 is true Gibbs-Bangham shrinkage, then a calculated value of 17 172 MPa (2.49×10^6 psi) would be obtained for the elastic modulus of the solid hydration products. This is based on an estimated value of 31 034 MPa (4.5×10^6 psi) for the solid hydration products including micropores.[29] In the present study the calculated elastic modulus values for the 0.4 and 0.6 W/C ratio pastes are 5605 MPa (0.81×10^6 psi) and 5878 MPa (0.85×10^6 psi), respectively. A density value of 2.23 g/cm^3 was assumed.[30] The surface areas for the hydration products of the 0.4 and 0.6 W/C ratio pastes were calculated at 68.8 and 94.3 m^2/g, respectively, based on measured values of 53 and 83 m^2/g. The measured values include unhydrated cement, however. The degrees of hydration were estimated from work by Taplin,[31] as cited by Soroka.[32] They are 79% and 89%. The values used for the pastes were obtained from Fig. 7, according to which λ is 27.5×10^{-1} and 35.7×10^{-1} cm/N for the 0.4 and 0.6 W/C ratio pastes, respectively. Thus according to the present results for the calculated elastic modulus, true Gibbs-Bangham shrinkage is approximately 33% of total Gibbs-Bangham stress-induced shrinkage. Consequently 67% of total first drying shrinkage is not true Gibbs-Bangham shrinkage.

(5) Capillary Stress Shrinkage

The shrinkage superimposed onto the Gibbs-Bangham stress shrinkage may be capillary stress shrinkage. This agrees with the *V-t* curve of the 0.6 W/C ratio paste which shows capillary condensation above 25% rh corresponding to t values greater than 0.54 nm. Capillary stress shrinkage is significantly less in the 0.4 W/C ratio paste, which is reasonable since less capillary pore volume is expected. In fact the nitrogen *V-t* curve suggests that there are no capillary pores of pore diameters up to about 70 nm, which is about the upper limit for nitrogen sorption. The nitrogen *V-t* desorption curve would most likely show some capillary effect which may be too small to be detected on the adsorption branch.

Table II. Pore Volume of 0.4 and 0.6 W/C Ratio Pastes Hydrated for 165 d

	V(MIP) (cm^3/g)	V_{N_2} (liq cm^3/g)	V(MIP) + V_{N_2} (cm^3/g)	V(water) (cm^3/g)
0.4 W/C	0.113	0.054	0.167	0.190
0.6 W/C	0.236	0.084	0.320	0.322

(6) Irreversible Shrinkage

It is difficult to establish the origin of nearly 67% of first drying shrinkage. It is probably tied to irreversible shrinkage. This is supported from shrinkage results by Helmuth and Turk[25] which show that irreversible shrinkage accounts for 60% or more of first drying shrinkage following long-term drying. Measurements of basal spacings from X-ray diffraction of crystalline calcium silicate hydrates have shown that there is a continuous decrease in basal spacing with decrease in relative humidity, and that most of this is irreversible.[33] It is suggested that in cement paste opposing interlayer surfaces acquire a closer proximity upon drying. This process may take place in areas characterized by a spacing greater or smaller than that of a monolayer of water and therefore does not require removal of interlayer water. Such movement would be largely irreversible.

(7) Validity of Using Nitrogen for External Surface Area Measurements

It can be seen from Table II that the pore volume from nitrogen sorption and MIP combined agrees very well with that of water even though nitrogen sorption measures only a fraction of the total external pore volume determined by water loss in the rh range of 100% to 0% (Figs. 2(*A*) and (*B*)). These volumes account for 88% and 99% of the pore volume by water of the 0.4 and 0.6 W/C ratio pastes, respectively, assuming that the density of all external water is 1.0 g/cm^3. The agreement would have been even better if the amount of interlayer water lost at low relative humidities could be accounted for and if a higher density for adsorbed water was used. MIP was used to obtain the volume of pores of 4 nm in pore diameter and larger. These curves are shown in Fig. 8. The volume of pores smaller than 4 nm in size was determined from nitrogen *V-t* curves (Fig. 5). This pore volume can be obtained from Eq. (5).

$$\sum V_{N_2} = V_t - V_c - V_s \quad (cm^3/g) \tag{5}$$

V_t is the total pore volume from the *V-t* curve at $t = 2$ nm. This would correspond to a pore size of 4 nm assuming slit-shaped pores. V_c is the cumulative condensation pore volume. V_s is the cumulative volume from multilayer adsorption in the pores larger than 4 nm. Although this occurs on curved surfaces (cylindrical pores), it can be approximated by adsorption on a plane surface. At $t = 2$ nm

$$V_s = 2S_p \times 10^{-3} \quad (cm^3/g) \tag{6}$$

where S_p is the surface area in m^2/g of pores greater than 4 nm in diameter. It is obtained from the slope of the tangent of the *V-t* curve at $t = 2$ nm. Thus nitrogen measures the true external surface area of cement paste, which has been solvent replaced. This agrees with results by Litvan[14] and is in general agreement with those of Feldman.[34]

IV. Conclusions

(1) From dynamic shrinkage-weight loss curves it is concluded that moisture gradients and duration of shrinkage stresses do not affect total shrinkage of thin specimens of portland cement paste. Thus true material shrinkage can be obtained.

(2) Two stress-active shrinkage mechanisms have been identified upon first drying. They are the Gibbs-Bangham (surface free energy) and the capillary tension mechanisms, of which Gibbs-Bangham is the major component. It is active in the rh range

between 100% and 0%, whereas the capillary stress mechanism is active in the rh range above 25%.

(3) Elastic modulus calculations of the hydration products show that "true" Gibbs-Bangham shrinkage can only account for about 33% of the Gibbs-Bangham stress-induced shrinkage.

(4) External pore volume calculations of solvent-replaced 0.4 and 0.6 W/C ratio pastes using nitrogen sorption and MIP show good agreement with total pore volume by water. Nitrogen, therefore, measures the external surface area.

Acknowledgments: The author gratefully acknowledges helpful discussions with Mr. Jamal A. Almudaiheem, Ph.D. Candidate, the University of Michigan, and Professors R. L. Berger and J. F. Young, the University of Illinois at Champaign-Urbana, Illinois.

References

[1]T. C. Powers, "The Mechanisms of Shrinkage and Reversible Creep of Hardened Cement Paste," *Proc. Int. Conf. Struct. Conc., London*, 319–44 (1965).
[2]T. C. Powers, "The Thermodynamics of Volume Change and Creep," *Mater. Struct.*, **1** [6] 487–507 (1968).
[3]R. F. Feldman, "Sorption and Length Change Scanning Isotherms of Methanol and Water on Hydrated Portland Cement," *Proc. Int. Symp. Chem. Cem., 5th, Tokyo, Part III*, 53–66 (1968).
[4]R. F. Feldman and P. J. Sereda, "Sorption of Water on Compacts of Bottle-Hydrated Cement, II. Thermodynamic Considerations and Theory of Volume Change," *J. Appl. Chem.*, **14**, 93–104 (1964).
[5]R. A. Helmuth, "Dimensional Changes and Water Adsorption of Hydrated Portland Cement and Tricalcium Silicate"; M.S. Thesis. Chicago Institute of Technology, Chicago, IL, 1965.
[6]L. J. Parrott and J. F. Young, "The Drying Shrinkage of Two Alite Pastes"; pp. 35–48 in Fundamental Research on Creep and Shrinkage of Concrete. Martinus Nijhoff Publishers, The Hague, The Netherlands, 1982.
[7]F. H. Wittmann, "Interaction of Hardened Cement Paste and Water," *J. Am. Ceram. Soc.*, **56** [8] 409–15 (1973).
[8]R. F. Feldman and P. J. Sereda, "A Model for Hydrated Portland Cement and Its Practical Implications," *Eng. J.*, **53** [8/9] 53–59 (1970).
[9]J. F. Young, R. L. Berger, and A. Bentur, "Shrinkage of Tricalcium Silicate Pastes: Superposition of Several Mechanisms," *Cemento*, **75** [3] 391–98 (1978).
[10]Z. P. Bazant, "Thermodynamics of Hindered Adsorption and Its Implications for Hardened Cement Paste and Concrete," *Cem. Concr. Res.*, **2** [1] 1–16 (1972).
[11]F. H. Wittman, "The Structure of Hardened Cement Paste—A Basis for a Better Understanding of the Materials Properties"; pp. 96–117. Cement and Concrete Association, London, England, 1976.
[12]R. F. Feldman and P. J. Sereda, "A Model for Hydrated Portland Cement Paste as Deduced from Sorption-Length Change and Mechanical Properties," *Mater. Constr. (Paris)*, **1** [6] 509–20 (1968).
[13]L. J. Parrott, W. Hansen, and R. L. Berger, "Effect of First Drying upon the Pore Structure of Hydrated Alite Paste," *Cem. Concr. Res.*, **10** [5] 647–55 (1980).
[14]C. G. Litvan, "Variability of the Nitrogen Surface Area of Hydrated Cement Paste," *Cem. Concr. Res.*, 139–44 (1976).
[15]R. W. Cranston and F. A. Inkley, "The Determination of Pore Structures from Nitrogen Adsorption Isotherms"; pp. 143–54 in Advances in Catalysis and Related Subjects, Vol. 9. Academic Press, New York, 1957.
[16]H. Roper, "Dimensional Change and Water Sorption Studies of Cement Paste," Symposium on the Structure of Portland Cement Paste and Concrete, *Highw. Res. Board, Spec. Rep.*, **90**, 74–83 (1966).
[17]G. J. Verbeck and R. A. Helmuth, "Structures and Physical Properties of Cement Paste"; pp. 1–32 in Proceedings of the 5th International Symposium on the Chemistry of Cement, Tokyo, 1968, Vol. III. Cement Association of Japan, Tokyo, 1969.
[18]R. F. Feldman and E. G. Swenson, "Volume Changes on First Drying of Hydrated Portland Cement with and without Admixtures," *Cem. Concr. Res.*, **5** [1] 25–35 (1975).
[19]S. Sabri and J. M. Illston, "Isothermal Drying Shrinkage and Wetting Swelling of Hardened Cement Paste," pp. 63–72 in Fundamental Research on Creep and Shrinkage of Concrete. Martinus Nijhjoff Publishers, 1982.
[20]D. H. Bangham, N. Fakhoury, and A. F. Mohamed, "The Swelling of Charcoal. II, Some Factors Controlling the Expansion Caused by Water, Benzene and Pyridine Vapors," *Proc. R. Soc. London, Ser. A*, **138**, 162 (1932).
[21]D. H. Bangham and R. I. Razouk, "Adsorption and the Wettability of Solid Surfaces," *Trans. Faraday Soc.*, **33**, 1463 (1937).
[22]H. Freundlich, Colloid and Capillary Chemistry; p. 46. Methuen, London, 1926.
[23]B. C. Lippens and J. H. de Boer, "Studies on Pore Systems in Catalysts V. The *V-t* Method," *J. Catal.*, **4**, 319–23 (1965).
[24]K. H. Hiller, "Strength Reduction and Length Changes in Porous Glass Caused by Water Vapor Adsorption," *J. Appl. Phys.*, **35** [5] 1622–28 (1964).
[25]R. A. Helmuth and D. H. Turk, "The Reversible and Irreversible Drying Shrinkage of Hardened Portland Cement and Tricalcium Silicate Paste," *J. PCA Res. Dev. Lab.*, **9** [2] 8–21 (1967).
[26]D. H. Bangham and F. A. P. Maggs, "The Strength and Elastic Constants of Coals in Relation to Their Ultra-fine Structure"; pp. 118–30 in International Proceedings of a Conference on the Ultrafine Structure of Coals and Cokes, British Coal Utilization Research Association, June 1943. H. K. Lewis and Co., Ltd., London.
[27]C. H. Amberg and R. McIntosh, "A Study of Adsorption Hysteresis by Means of Length Changes of a Rode of Porous Glass," *Can. J. Chem.*, 1012–32 (1952).
[28]International Critical Tables, Vol. 2; p. 93. McGraw-Hill, New York, 1927.
[29]R. A. Helmuth and D. H. Turk, "Elastic Moduli of Hardened Portland Cement and Tricalcium Silicate Pastes: Effect of Porosity," *Highw. Res. Board, Spec. Rep.*, **90**, 135–44 (1966).
[30]R. F. Feldman, "Density and Porosity Studies of Hydrated Portland Cement," *Cem. Technol.*, **3**, 5–14 (1972).
[31]J. H. Taplin, "A Method for Following the Hydration Reaction in Portland Cement Paste," *Aust. J. Appl. Sci.*, **10**, 329–45 (1959).
[32]I. Soroka, Portland Cement Paste and Concrete, p. 40; pp. 1–338. Macmillan Press Ltd., London, 1979.
[33]W. A. Gutteridge and L. J. Parrott, "A Study of the Changes in Weight, Length and Interplanar Spacing Induced by Drying and Rewetting Synthetic CSH(I)," *Cem. Concr. Res.*, **6**, 357–66 (1976).
[34]R. F. Feldman, "Assessment of Experimental Evidence for Models of Hydrated Portland Cement," *Highw. Res. Rec.*, **370**, 8–24 (1971). □